Available online at www.sciencedirect.com

ScienceDirect

Nuclear Physics B 975 (2022) 115665

NUCLEAR PHYSICS B

www.elsevier.com/locate/nuclphysb

Estimating the final spin of binary black holes merger in STU supergravity

Shou-Long Li [a], Wen-Di Tan [b,*], Puxun Wu [a], Hongwei Yu [a]

[a] *Department of Physics and Synergetic Innovation Center for Quantum Effects and Applications, Hunan Normal University, Changsha, Hunan 410081, China*

[b] *Center for Joint Quantum Studies and Department of Physics, School of Science, Tianjin University, Tianjin 300350, China*

Received 28 September 2021; received in revised form 10 December 2021; accepted 10 January 2022
Available online 17 January 2022
Editor: Stephan Stieberger

Abstract

In this paper, we adopt the so-called Buonanno-Kidder-Lehner (BKL) recipe to estimate the final spin of a rotating binary black hole merger in STU supergravity. According to the BKL recipe, the final spin can be viewed as the sum of the individual spins plus the orbital angular momentum of the binary system which could be approximated as the angular momentum of a test particle orbiting at the innermost stable circular orbit around the final black hole. Unlike previous works, we consider the contribution of the orbital angular momentum of the binary system to the final spin by requiring the test particle to preserve the scaling symmetry in the Lagrangian of supergravity. We find some subtle differences between two cases corresponding to whether the symmetry is taken into account or not. In the equal initial spin configuration, when the initial black holes are non-spinning, the final spin of the merger is always larger than that in the case in which the symmetry is not imposed although the general behaviors are similar. The difference increases firstly and then decreases as the initial mass ratio approaches unity. Besides, as the initial spins exceed a threshold, the final spin is always smaller than that in the case where the scaling symmetry is not considered. The difference decreases constantly as the equal initial mass limit is approached. All these features exist in the merger of a binary STU black hole with different charge configurations. We also study the final spin's difference between different charge configurations and different initial spin configurations.

* Corresponding author.
E-mail addresses: shoulongli@hunnu.edu.cn (S.-L. Li), TWDHANNAH@163.com (W.-D. Tan), pxwu@hunnu.edu.cn (P. Wu), hwyu@hunnu.edu.cn (H. Yu).

https://doi.org/10.1016/j.nuclphysb.2022.115665

1. Introduction

The evolution of the coalescence of a binary black hole (BBH) system is widely accepted to include three stages: inspiral, merger and ringdown. The early inspiral and ringdown stages can be well explained by the post-Newtonian approximation [1] and the black hole perturbation theory [2–5], respectively. Since the late inspiral and merger stages are highly nonlinear, only numerical relativity simulations could provide an accurate description of the dynamical properties of the whole process [6]. The numerical simulations have been widely used in the study of the discovered gravitational-wave (GW) events, such as those in Refs. [7–11]. However, full simulations have been known to be highly-costly, and take a lot of time. This inspires one to look for some reliable though may-not-so-rigorous methods to reproduce reasonably accurate results compared with those from available numerical simulations. One expects that such a method not only can give some useful predictions for the final state, but also is helpful to providing an accurate analytic template. In this regard, the Buonanno-Kidder-Lehner (BKL) recipe [12] provides a simple first-principles-derived method to estimate the final spin of the merger which is one of the most important properties of the remnant black hole that could help detection [13,14] and distinguish the BBH from other exotic objects [15]. The advantage of the recipe is that it can be applied to the merger of a BBH with arbitrary initial masses and spins. Based on the approximate conservation of mass and angular momentum of a BBH system during the merger and ringdown phases, and some other simple assumptions, the BKL recipe can be used to straightforwardly and accurately estimate the final angular momentum as a sum of the individual spins plus the orbital angular momentum of the binary system which could be approximated as the angular momentum of a test particle orbiting at the innermost stable circular orbit (ISCO) around the final rotating black hole. This point-particle approximation captures the key aspects of two-body dynamics, and the method is also supported by the numerical simulations [16–24].

By considering that the test particle is charged, the BKL recipe has been generalized to estimate the final spin of the binary charged black hole merger in the Einstein-Maxwell (EM) theory [25], as well as in the Kaluza-Klein (KK) theory [25] and the low energy limit of the heterotic string theory [26]. With the BKL recipe, the estimates for the final spin of a binary black hole merger in different modified gravities are expected to be different, and thus could be constrained by the observations. Although recent observations have been found to support general relativity, some subtle deviations may be probed as the higher signal-to-noise ratio will be achieved in the near future. So, the final spin of a BBH merger may provide a possible way to test the string theory and other modified gravities near strong gravitational regimes.

In this work, we would like to revisit the details of the generalized BKL recipe to estimate the final spins of a binary charged black hole merger. In the previous work [25], the Lagrangian of the charged test particle in the KK theory is taken the same as that in EM theory. However, it is worth noting that symmetry plays a very important role when we study the black hole in the framework of string theory and supergravities [27–29]. For example, after performing a dimensional reduction [30,31] on S^1 from five-dimensional pure Einstein gravity, the resulting four-dimensional Einstein-Maxwell-dilaton theory with a special coupling constant, i.e. the KK theory, has an extra scaling symmetry, namely a constant shift of the dilaton accompanied by an appropriate constant scaling of the Maxwell potential. This symmetry can be understood in terms of $\mathbb{R}^n (n = 1)$ [32]. If we further reduce the four-dimensional KK theory to the three-dimensional theory, the corresponding global symmetry $SL(3, R)$ can help us to explore solutions of the KK theory. So, it is worth examining the outcome from the BKL recipe when the Lagrangian describing the motion of the test particle also preserves the same symmetry [33]. In this case, the

angular momentum of the test particle may be modified. It is natural to ask whether the revised method could improve the precision of the estimation by comparing with the numerical simulations [34,35]. As a first step, we will study the difference of the final spin estimations between the two cases, i.e., the case where the scaling symmetry is taken into account and the one which is not.

On the other hand, it is worth noting that compared with Kerr-Newman (KN) black hole in EM theory, black holes in supergravities and string theory have extra scalar charges. When we study the binary dynamics in supergravities and string theory, it is necessary to consider the effects of scalar fields [33] apart from those of electromagnetic fields and gravitational fields. This could be achieved by writing the Lagrangian of test particle in an appropriate metric frame.

The four-dimensional EM theory, the KK theory and the low energy limit of the heterotic string theory can be viewed as the special cases of a more general supergravity, i.e. STU supergravity [32,36–38], which has an $SL(2,R)^3$ symmetry and also the so-called "S-T-U" triality symmetry under permutations of the three $SL(2,R)$ factors, and can be obtained from higher dimensional string theory and carries four independent electromagnetic fields. To be specific, STU rotating black holes carrying four equal charges, two equal charges and a single charge are equivalent to the KN black hole, the Einstein-Maxwell-dilaton-axion (EMDA) black hole (which is equivalent to Kerr-Sen black hole in the low energy limit of the heterotic string theory) [39] and the KK black hole [40] respectively. Here we will estimate the final spin of the binary STU black hole merger by using the BKL recipe and requiring the Lagrangian of the test particle to preserve the scaling symmetry in STU supergravity. Let us note here that a binary charged black hole could possibly be the source to produce the counterpart electromagnetic signal to the merger of BBH, which could be used to explain the signal recently observed by the Fermi Gamma-ray Burst Monitor (GBM) group [41–46]. So it is meaningful to explore the final spin of the merger of a binary charged black hole, at least BBH with weak charges ($Q \ll M$).

The organization of the paper is as follows. In section 2, we review the rotating black hole in the four-dimensional STU supergravity. In section 3, we review the BKL recipe and reconsider the contribution of the orbital angular momentum of the binary system to the final spin by requiring the test particle to preserve the scaling symmetry in STU supergravities. In section 4, we first study the ISCO of the test particle, and then estimate the final spin of binary STU rotating black holes with different charge configurations in different initial spin cases such as equal initial spins, unequal initial spins and generic initial spins. We conclude in section 5.

2. STU supergravity

The four-dimensional Lagrangian for the bosonic sector of the $\mathcal{N}=2$ supergravity coupled to three vector multiplets, also called the STU model, is given by [32,37,38]

$$\begin{aligned} L_{\rm STU} = R\star\mathbb{1} - \frac{1}{2}\sum_{i=1}^{3}(\star d\varphi_i\wedge d\varphi_i + e^{2\varphi_i}\star d\psi_i\wedge d\psi_i) - \frac{1}{2}e^{-\varphi_1}\big(e^{\varphi_2-\varphi_3}\star\hat{F}_1\wedge\hat{F}_1 \\ + e^{\varphi_2+\varphi_3}\star\hat{F}_2\wedge\hat{F}_2 + e^{-\varphi_2+\varphi_3}\star\hat{\mathcal{F}}^1\wedge\hat{\mathcal{F}}^1 + e^{-\varphi_2-\varphi_3}\star\hat{\mathcal{F}}^2\wedge\hat{\mathcal{F}}^2\big) \\ - \psi_1\big(\hat{F}_1\wedge\hat{\mathcal{F}}^1 + \hat{F}_2\wedge\hat{\mathcal{F}}^2\big), \end{aligned} \tag{2.1}$$

where φ_i and ψ_i are dilatons and axions respectively. The four field strengths can be written in terms of potentials as

$$\hat{F}_1 = d\hat{A}_1 - \psi_2 d\hat{\mathcal{A}}^2, \quad \hat{F}_2 = d\hat{A}_2 + \psi_2 d\hat{\mathcal{A}}^1 - \psi_3 d\hat{A}_1 + \psi_2\psi_3 d\hat{\mathcal{A}}^2,$$

$$\hat{\mathcal{F}}^1 = d\hat{\mathcal{A}}^1 + \psi_3 d\hat{\mathcal{A}}^2\,, \quad \hat{\mathcal{F}}^2 = d\hat{\mathcal{A}}^2\,. \tag{2.2}$$

The rotating STU black hole solution is given by [37]

$$\begin{aligned}
ds^2 &= -\frac{\rho^2 - 2mr}{W}(dt + \mathcal{B})^2 + W\left(\frac{dr^2}{\Delta} + d\theta^2 + \frac{\Delta \sin^2\theta d\phi^2}{\rho^2 - 2mr}\right),\\
\hat{A}_1 &= A_1 + \sigma_1\mathcal{B} + \sigma_1 dt\,, \quad \hat{A}_2 = A_2 + \sigma_2\mathcal{B} + \sigma_2 dt\,,\\
\hat{\mathcal{A}}^1 &= \mathcal{A}^1 + \sigma_3\mathcal{B} + \sigma_3 dt\,, \quad \hat{\mathcal{A}}^2 = \mathcal{A}^2 + \sigma_4\mathcal{B} + \sigma_4 dt\,,\\
\psi_1 &= \frac{2mu(c_{13}s_{24} - c_{24}s_{13})}{r_1 r_3 + u^2}\,, \quad \psi_2 = \frac{2mu(c_{14}s_{23} - c_{23}s_{14})}{r_2 r_3 + u^2}\,,\\
\psi_3 &= \frac{2mu(c_{12}s_{34} - c_{34}s_{12})}{r_1 r_2 + u^2}\,,\\
\varphi_1 &= \ln\frac{r_1 r_3 + u^2}{W}\,, \quad \varphi_2 = \ln\frac{r_2 r_3 + u^2}{W}\,, \quad \varphi_3 = \ln\frac{r_1 r_2 + u^2}{W}\,,
\end{aligned} \tag{2.3}$$

where

$$\begin{aligned}
\mathcal{B} &= \frac{2m(a^2 - u^2)(rc_{1234} - (r-2m)s_{1234})}{a(\rho^2 - 2mr)}d\phi\,,\\
A_1 &= -\frac{2muc_1 s_1 \Delta d\phi}{a(\rho^2 - 2mr)}\,, \quad A_2 = -\frac{2mu(a^2 - u^2)((r-2m)c_2 s_{134} - rc_{134}s_2)d\phi}{a(\rho^2 - 2mr)}\,,\\
\mathcal{A}^1 &= -\frac{2muc_3 s_3 \Delta d\phi}{a(\rho^2 - 2mr)}\,, \quad \mathcal{A}^2 = -\frac{2mu(a^2 - u^2)((r-2m)c_4 s_{123} - rc_{123}s_4)d\phi}{a(\rho^2 - 2mr)}\,,\\
\sigma_1 &= \frac{2mu}{W^2}\left((rr_1 + u^2)(c_{234}s_1 - s_{234}c_1) + 2mr_1 s_{234}c_1\right),\\
\sigma_2 &= \frac{1}{W^2}\left(2mc_2 s_2(r_1 r_3 r_4 + ru^2) + 4m^2u^2 e_2\right),\\
\sigma_3 &= \frac{2mu}{W^2}\left((rr_3 + u^2)(c_{124}s_3 - s_{124}c_3) + 2mr_3 s_{124}c_3\right),\\
\sigma_4 &= \frac{1}{W^2}\left(2mc_4 s_4(r_1 r_2 r_3 + ru^2) + 4m^2u^2 e_4\right),\\
e_2 &= c_{134}s_{134}(c_2^2 + s_2^2) - c_2 s_2(s_{13}^2 + s_{14}^2 + s_{34}^2 + s_{134}^2)\,,\\
e_4 &= c_{123}s_{123}(c_4^2 + s_4^2) - c_4 s_4(s_{12}^2 + s_{13}^2 + s_{23}^2 + s_{123}^2)\,,\\
W^2 &= \prod_{i=1}^4 r_i + u^4 + 2u^2\left(r^2 + mr\sum_{i=1}^4 s_i^2 + 4m^2(\prod_{i=1}^4 c_i s_i - \prod_{i=1}^4 s_i^2) - 2m^2\sum_{i<j<k}^4 s_i^2 s_j^2 s_k^2\right),\\
\Delta &= r^2 - 2mr + a^2\,, \quad \rho^2 = r^2 + a^2\cos^2\theta\,, \quad r_i = r + 2ms_i^2\,, \quad u = a\cos\theta\,,\\
c_{1\ldots n} &= \cosh\delta_1 \ldots \cosh\delta_n\,, \quad s_{1\ldots n} = \sinh\delta_1 \ldots \sinh\delta_n\,,
\end{aligned} \tag{2.4}$$

where parameters $(m, a, \delta_1, \delta_2, \delta_3, \delta_4)$ characterize mass, angular momentum, and four electric charges respectively.

The four-dimensional theory (2.1), which can be obtained from the one in six-dimensions by reducing the bosonic string on T^2, has a global symmetry $SL(2,\mathbb{R})^3$, realized nonlinearly on the scalar coset $(SL(2,\mathbb{R})/U(1))^3$ [37]. It is worth noticing that the local general coordinate symmetry in the six-dimensional bosonic string involves coordinate reparameterizations by arbitrary

functions of six coordinates, while the local general coordinate symmetry and $U(1)$ gauge transformations in four dimensions involve arbitrary functions of only four coordinates. Actually the theory has another symmetry, namely a constant shift of the dilaton fields φ_i, accompanied by an appropriate constant scaling of the axion fields ψ_i and the Maxwell potentials:

$$\begin{aligned}
&\varphi_1 \to \varphi_1 + \alpha_1\,, \quad \varphi_2 \to \varphi_2 + \alpha_2\,, \quad \varphi_3 \to \varphi_3 + \alpha_3\,,\\
&\psi_1 \to \psi_1 e^{-\alpha_1}\,, \quad \psi_2 \to \psi_2 e^{-\alpha_2}\,, \quad \psi_1 \to \psi_3 e^{-\alpha_3}\,,\\
&\hat{A}_1 \to \hat{A}_1 e^{\frac{\alpha_1-\alpha_2+\alpha_3}{2}}\,, \quad \hat{A}_2 \to \hat{A}_2 e^{\frac{\alpha_1-\alpha_2-\alpha_3}{2}}\,,\\
&\hat{\mathcal{A}}^1 \to \hat{\mathcal{A}}^1 e^{\frac{\alpha_1+\alpha_2-\alpha_3}{2}}\,, \quad \hat{\mathcal{A}}^2 \to \hat{\mathcal{A}}^2 e^{\frac{\alpha_1+\alpha_2+\alpha_3}{2}}\,,
\end{aligned} \tag{2.5}$$

which is important to studying the supergravity and the solutions of the theory. For our purpose to study the binary STU black hole merger, we would also like to consider the effect of the symmetry on the final spin estimation of the remnant black hole. For simplicity, we focus on some special cases of the binary STU rotating black holes with different charge configurations. First, we consider the STU rotating black hole with a single non-zero charge, i.e. $\delta_4 = \delta \neq 0$ ($\sinh\delta = s, \cosh\delta = c$), $\delta_1 = \delta_2 = \delta_3 = 0$. The solution reduces to the KK rotating black hole (the full solution is given in the Appendix A), and the corresponding theory is described by

$$\mathcal{L}_{\rm KK} = R - \frac{1}{2}(\nabla\varphi)^2 - \frac{1}{4}e^{-\sqrt{3}\varphi}F^2\,, \tag{2.6}$$

where the canonically-normalized electromagnetic field $F = \mathcal{F}^2$, $\varphi = \sqrt{3}\varphi_1 = \sqrt{3}\varphi_2 = \sqrt{3}\varphi_3$, $\psi_1 = \psi_2 = \psi_3 = 0$, $\mathcal{F}^1 = F_1 = F_2 = 0$, and we have for the physical mass M, charge Q, and angular momentum J,

$$M = \frac{m}{2}(2 + s^2)\,, \quad Q = \frac{msc}{2}\,, \quad J = mac\,. \tag{2.7}$$

The corresponding scaling symmetry is given by

$$\varphi \to \varphi + \alpha\,, \quad A \to A e^{\frac{\sqrt{3}}{2}\alpha}\,. \tag{2.8}$$

Second, we consider the STU rotating black hole with two non-zero equal charges, i.e. $\delta_2 = \delta_4 = \delta \neq 0, \delta_1 = \delta_3 = 0$. The solution reduces to the EMDA rotating black hole (the full solution is given in the Appendix A), and the corresponding theory is governed by

$$\mathcal{L}_{\rm EMDA} = R - \frac{1}{2}(\nabla\varphi)^2 - \frac{1}{2}e^{2\varphi}(\nabla\psi)^2 - \frac{1}{4}e^{-\varphi}F^2 - \frac{1}{8}\psi\epsilon^{\mu\nu\rho\sigma}F_{\mu\nu}F_{\rho\sigma}\,, \tag{2.9}$$

where $\epsilon^{\mu\nu\rho\sigma}$ is the Levi-Civita tensor, the canonically-normalized electromagnetic field $F = \mathcal{F}^2/\sqrt{2} = F_2/\sqrt{2}$, $\varphi = \varphi_1$, $\psi = \psi_1$, $\mathcal{F}^1 = F_1 = 0$, $\varphi_2 = \varphi_3 = 0$, $\psi_2 = \psi_3 = 0$, and we have

$$M = mc^2\,, \quad Q = \frac{\sqrt{2}}{2}msc\,, \quad J = mc^2 a\,. \tag{2.10}$$

The corresponding scaling symmetry reduces to

$$\varphi \to \varphi + \alpha\,, \quad A \to A e^{\frac{1}{2}\alpha}\,, \quad \psi \to \psi e^{-\alpha}\,. \tag{2.11}$$

Third, we consider the STU rotating black hole with four non-zero equal charges, i.e. $\delta_1 = \delta_2 = \delta_3 = \delta_4 = \delta \neq 0$, the solution reduces to the KN black hole (the full solution is given in the Appendix A) after making a coordinate transformation $r \to r + 2ms^2$ and applying the electromagnetic duality, and the corresponding theory is described by

$$\mathcal{L}_{\rm EM} = R - \frac{1}{4}F^2\,, \tag{2.12}$$

where the canonically-normalized electromagnetic field $F = \mathcal{F}^1 = F_1 = \mathcal{F}^2 = F_2, \varphi_1 = \varphi_2 = \varphi_3 = 0, \psi_1 = \psi_2 = \psi_3 = 0$, and we have

$$M = m(s^2 + c^2)\,, \quad Q = msc\,, \quad J = m(s^2 + c^2)a\,. \tag{2.13}$$

There is no similar scaling symmetry in the EM theory because all of the dilatons and axions vanish.

3. BKL recipe in STU supergravity

In this section we will first review the BKL recipe and consider the contribution of the orbital angular momentum of the binary system to the final spin by requiring the Lagrangian of the test particle to preserve the scaling symmetry mentioned before. Then we will examine the Newtonian limit of the motion of the test particle orbiting the final black hole.

The BKL recipe [12] was proposed to estimate the final spin of a BBH merger with arbitrary initial masses and spins based on first principles and a few safe assumptions. One assumes that the BBH system evolves quasi-adiabatically, and radiates much angular momentum, which causes the binary orbit to become smaller gradually during the inspiral stage until it reaches the ISCO. Once the ISCO radius is reached, the binary orbit becomes unstable and a "plunge" occurs, resulting in the BBH merger, and then the final black hole forms quickly. The loss of mass and angular momentum with respect to the total mass and angular momentum of the binary system is small during the merger stage, and so it is reasonable to argue that mass and angular momentum are conserved approximately. One can also assume that the magnitude of the individual spins of the black holes remains constant because both spin-spin and spin-orbit couplings are small, and the radiation falling into the black holes affects the spins by a small amount. Therefore, the mass M of the final black hole can be given by

$$M = M_1 + M_2\,, \tag{3.1}$$

where M_1 and M_2 are the masses of initial black holes. The final mass M can also be described by a more accurate expression [47]. As mentioned before, the loss of the mass is small during the whole stages and this is a good approximation to the first order in the gravitational wave observations [7–11]. Moreover, the contribution of the orbital angular momentum to the final angular momentum of the black hole remnant can be described by the angular momentum of a test particle orbiting around the final rotating black hole at ISCO. The conservation of angular momentum at the moment of plunge implies that

$$M\mathcal{A}_f = L_{\rm orb} + M_1\mathcal{A}_1 + M_2\mathcal{A}_2\,, \tag{3.2}$$

where $\mathcal{A}_f$ is the spin of the final black hole, $\mathcal{A}_1$ and $\mathcal{A}_2$ are spins of initial black holes, and $L_{\rm orb}$ is the orbital angular momentum of the binary system which is represented by the angular momentum of a test particle with reduced mass $\mu = M_1M_2/M$ orbiting around the final black hole at ISCO. The final spin can be written as

$$\mathcal{A}_f = \mathcal{L}\nu + \frac{M\chi_1}{4}(1 + \sqrt{1-4\nu})^2 + \frac{M\chi_2}{4}(1 - \sqrt{1-4\nu})^2\,, \tag{3.3}$$

where $\mathcal{L} = L_{\rm orb}/\mu$ is the angular momentum of the test particle with unit mass, $\chi_i = A_i/M_i (i = 1, 2)$, and $\nu = \mu/M$.

The contribution of the orbital angular momentum of the binary charged black hole to the final spin can be effectively described by the angular momentum of a charged test particle orbiting around the final black hole [25]. Furthermore, it is worth considering that the charged test particle preserves the symmetry in the Lagrangian of gravities when we discuss the particle motion in the framework of supergravity [33]. Once the symmetry is taken into account, the particle motion and the orbital angular momentum are expected to be modified. Now we examine the Newtonian limit and identify reasonable mass and charge assignments for our consideration.

Generically, the motion of a relativistic particle of mass μ coupled to the Maxwell field A with charge q is governed by the action

$$\mathcal{S}_0 = \int d\tau \left(-\mu \sqrt{-g_{\lambda\nu} \dot{X}^\lambda \dot{X}^\nu} - \frac{1}{4} q A_\nu \dot{X}^\nu \right) , \tag{3.4}$$

where τ and X represent the proper time and coordinate respectively, and the dot denotes the derivative with respect to τ. For our purpose to consider the test particle that preserves the symmetry, the action should be given by [33]

$$\mathcal{S}_1 = \int L_1 d\tau = \int d\tau \left(-\mu \sqrt{-e^{\beta\varphi} g_{\lambda\nu} \dot{X}^\lambda \dot{X}^\nu} - \frac{1}{4} q A_\nu \dot{X}^\nu \right) . \tag{3.5}$$

Compared with $\mathcal{S}_0$, the action $\mathcal{S}_1$ has the symmetry

$$\varphi \to \varphi + \alpha \,, \quad A_\nu \to A_\nu e^{\frac{1}{2}\alpha\beta} \,. \tag{3.6}$$

It is worth noting that this type of symmetry is akin to a homothety. Under the homothetic transformation (3.6), the action $\mathcal{S}_1$ will have an overall factor $e^{\alpha\beta/2}$. In order to match the symmetry in previous cases, the values of β are

$$\text{KK} : \beta = \sqrt{3} \,, \quad \text{EMDA} : \beta = 1 \,, \quad \text{EM} : \beta = 0 \,. \tag{3.7}$$

The related geodesic equation becomes

$$\mu \left(\ddot{X}^\mu + \Gamma^\mu{}_{\rho\sigma} \dot{X}^\rho \dot{X}^\sigma \right) - \frac{\mu\beta}{2} (\partial^\mu \varphi + \partial_\lambda \varphi \dot{X}^\lambda \dot{X}^\mu) = \frac{1}{4} q e^{-\frac{1}{2}\alpha\beta} \dot{X}^\nu F_\nu{}^\mu \tag{3.8}$$

which is invariant under the transformation (3.6). Note that the action $\mathcal{S}_1$ is difficult to quantize because it contains a square root, and cannot be used to describe a massless particle. Classically, this action $\mathcal{S}_1$ is equivalent to

$$\mathcal{S}_2 = \int L_2 d\tau = \int d\tau \left(\frac{1}{2} \xi^{-1} e^{\beta\varphi} g_{\lambda\nu} \dot{X}^\lambda \dot{X}^\nu - \frac{1}{2} \mu^2 \xi - \frac{1}{4} q A_\nu \dot{X}^\nu \right) . \tag{3.9}$$

where $\xi(\tau)$ is the auxiliary field. The homothetic symmetry for action $\mathcal{S}_2$ becomes

$$\varphi \to \varphi + \alpha \,, \quad A_\nu \to A_\nu e^{\frac{1}{2}\alpha\beta} \,, \quad \xi \to \xi e^{\frac{1}{2}\alpha\beta} \,. \tag{3.10}$$

We can introduce a new metric

$$\tilde{g}_{\lambda\nu} = e^{\beta\varphi} g_{\lambda\nu} \,, \tag{3.11}$$

where the conformal factor $e^{\beta\varphi}$ takes into account precisely the effect of the dilaton. The weights of $(\tilde{g}_{\lambda\nu}, \tilde{g}^{\lambda\nu}, A_\nu, A^\nu, \xi)$ are $(1, -1, 1/2, -1/2, 1/2)$, respectively. Here $\tilde{g}^{\lambda\nu}$ and $\tilde{g}_{\lambda\nu}$ have opposite weights, and we will let $\tilde{g}^{\lambda\nu}$ and $\tilde{g}_{\lambda\nu}$ raise and lower the indexes in the remaining discussions. By varying the action $\mathcal{S}_2$ with respect to the auxiliary field ξ, the corresponding equation of motion is found to be

$$\xi^2\mu^2 + \tilde{g}_{\lambda\nu}\dot{X}^\lambda\dot{X}^\nu = 0\,. \tag{3.12}$$

Solving the above equation for ξ and substituting the solution back into $\mathcal{S}_2$ gives the original action $\mathcal{S}_1$. Varying both actions $\mathcal{S}_1$ and $\mathcal{S}_2$ with respect to X^μ yields the same equation of motion

$$\mu\left(\ddot{X}^\lambda + \tilde{\Gamma}^\lambda{}_{\rho\sigma}\dot{X}^\rho\dot{X}^\sigma\right) = \frac{1}{4}q\dot{X}^\nu\tilde{F}_\nu{}^\lambda\,, \tag{3.13}$$

where $\tilde{\Gamma}^\lambda{}_{\rho\sigma}$ denotes the affine connection defined by the metric $\tilde{g}_{\mu\nu}$. Here we have chosen a gauge for the shifting symmetry (3.6) such that $\tilde{g}_{\lambda\nu}\dot{X}^\lambda\dot{X}^\nu = -1$. Notice that we consider the binary STU black holes carrying a small amount of charges ($Q \ll M$). To be specific, we consider the STU black holes with a single charge (KK), two equal charges (EMDA), and four equal charges (KN). Substituting the solutions (A.1), (A.3) and (A.5) into above equation, and expressing the resulting equation in terms of the physical mass M and charge Q, one can obtain the same standard radial equation of motion

$$\mu\left(\frac{d^2r}{dt^2} + \frac{M}{r^2}\right) = \frac{qQ}{r^2}\,, \tag{3.14}$$

for different values of β by imposing the Newtonian limit conditions. This can be seen as the equation of motion of two interacting charged massive particles

$$\frac{M_1M_2}{M_1+M_2}\frac{d^2r}{dt^2} + \frac{M_1M_2}{r^2} = \frac{Q_1Q_2}{r^2}\,, \tag{3.15}$$

where $\mu = M_1M_2/M$ and $q = Q_1Q_2/Q$ can be seen as the reduced mass and the charge of the test particle. We have now identified the mass and charge assignments for the BKL recipe by imposing the scaling symmetry in supergravities.

4. Final spin estimation

Now we apply the BKL recipe to estimate the final spin of merger of a binary rotating STU black hole with different charge configurations and different initial spin configurations, i.e., equal initial spins, unequal initial spins, and general initial spins. As the first step in exploring whether the revised method could improve the precision of estimation, we will study the final spin's difference between two cases corresponding to whether the scaling symmetry is taken into account or not.

4.1. ISCO

As mentioned before, the particle motion will be modified if the scaling symmetry is taken into consideration. We will study the ISCO which is related to the test particle motion. The conjugate momentum with respect to X^λ is given by

$$P_\lambda = \frac{\partial L_2}{\partial\dot{X}^\lambda} = \frac{\mu\tilde{g}_{\lambda\nu}\dot{X}^\nu}{\sqrt{-\tilde{g}_{\lambda\nu}\dot{X}^\lambda\dot{X}^\nu}} - \frac{1}{4}qA_\lambda = \mu\tilde{g}_{\lambda\nu}\dot{X}^\nu - \frac{1}{4}qA_\lambda\,, \tag{4.1}$$

where we have used the gauge

$$\tilde{g}_{\mu\nu}\dot{X}^\mu\dot{X}^\nu = -1 = \tilde{g}_{tt}\dot{t}^2 + \tilde{g}_{rr}\dot{r}^2 + \tilde{g}_{\theta\theta}\dot{\theta}^2 + \tilde{g}_{\phi\phi}\dot{\phi}^2 + 2\tilde{g}_{t\phi}\dot{t}\dot{\phi}\,, \tag{4.2}$$

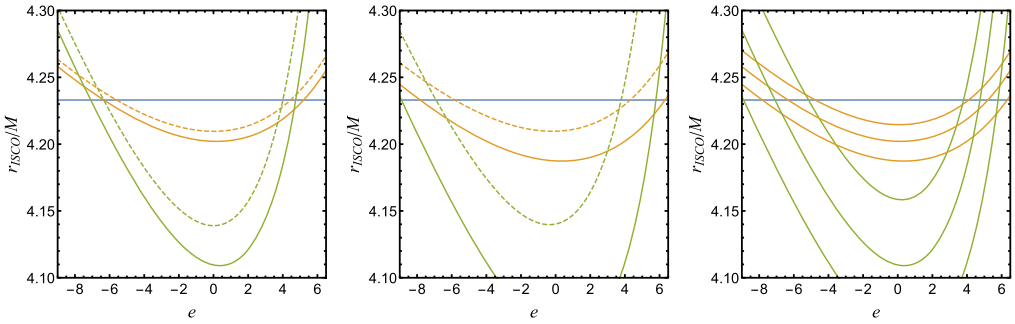

Fig. 1. The radius $r_{\rm ISCO}/M$ against the charge to mass ratio e in different cases. We set $A_f = 0.5M$ for simplicity. The blue, orange and green lines represent the $Q = 0$, $Q = 0.05M$, and $Q = 0.1M$ cases respectively. The solid lines represent the cases in which the Lagrangian of test particle preserves the scaling symmetry, and the dashed lines represent the cases in which the symmetry is not imposed. Left: EMDA; middle: KK; right: the lines in same color represent the KN, EMDA and KK cases respectively from top to bottom.

Now we consider the motion of a charged massive particle in the equatorial plane of the KK rotating black hole, determined by $\theta = \pi/2$ and $\dot{\theta} = 0$. The energy $\mathcal{E}$ and angular momentum $\mathcal{L}$ of the test particle with unit mass are given by

$$\mathcal{E} = -\frac{P_t}{\mu} = -\tilde{g}_{tt}\dot{t} - \tilde{g}_{t\phi}\dot{\phi} + \frac{1}{4}eA_t\,, \tag{4.3}$$

$$\mathcal{L} = \frac{P_\phi}{\mu} = \tilde{g}_{\phi\phi}\dot{\phi} + \tilde{g}_{t\phi}\dot{t} - \frac{1}{4}eA_\phi\,, \tag{4.4}$$

where $e = q/\mu$ represents the charge to mass ratio of the test particle. We can obtain

$$\dot{t} = \frac{(4\mathcal{L} + eA_\phi)\tilde{g}_{t\phi} + (4\mathcal{E} - eA_t)\tilde{g}_{\phi\phi}}{4\tilde{\Delta}_r}\,, \tag{4.5}$$

$$\dot{\phi} = -\frac{(4\mathcal{L} + eA_\phi)\tilde{g}_{tt} + (4\mathcal{E} - eA_t)\tilde{g}_{t\phi}}{4\tilde{\Delta}_r}\,, \tag{4.6}$$

where $\tilde{\Delta}_r = \tilde{g}_{t\phi}^2 - \tilde{g}_{tt}\tilde{g}_{\phi\phi}$. Substituting Eqs. (4.5) and (4.6) into (4.2), we can define the effective potential

$$V_{\rm eff} \equiv \dot{r}^2 = \frac{(4\mathcal{L} + eA_\phi)^2\tilde{g}_{tt} + (4\mathcal{E} - eA_t)^2\tilde{g}_{\phi\phi} + 2(4\mathcal{L} + eA_\phi)(4\mathcal{E} - eA_t)\tilde{g}_{t\phi} - 16\tilde{\Delta}_r}{16\tilde{\Delta}_r\tilde{g}_{rr}}\,. \tag{4.7}$$

The ISCO can be found by imposing the following conditions

$$V_{\rm eff} = 0\,, \quad V'_{\rm eff} = 0\,, \quad V''_{\rm eff} = 0\,, \tag{4.8}$$

where the prime denotes the derivative with respect to r. We plot the $r_{\rm ISCO}$ against e in the EMDA and KK cases in Fig. 1. First, as the charge to mass ratio e varies from negative to positive, the ISCO radius gradually reduces to a minimal value, and then begins to increase if the black hole carries nonzero charge. Second, we find that the ISCO radius will be smaller when we require the test particle to preserve the scaling symmetry in both KK and EMDA cases. As the black hole carries more charges, the difference becomes larger of the ISCO radius between two cases corresponding to whether the symmetry is taken into account or not. From the right

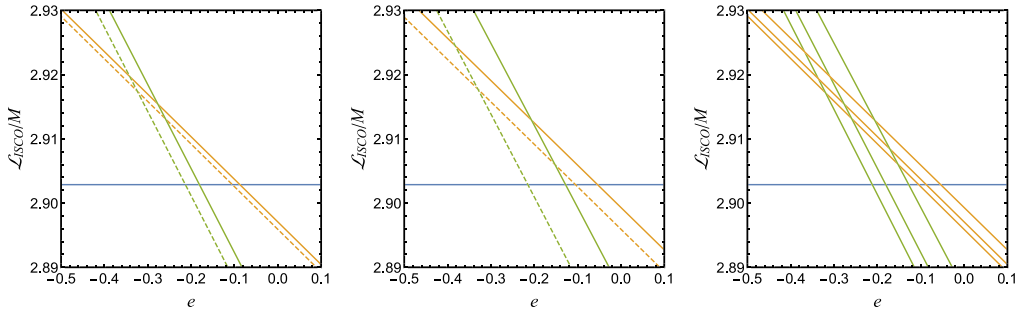

Fig. 2. The angular momentum of the test particle with unit mass $\mathcal{L}_{\rm ISCO}/M$ against the charge to mass ratio e in different cases. We set $A_f = 0.5M$. The blue, orange and green lines represent the $Q = 0$, $Q = 0.05M$, and $Q = 0.1M$ cases respectively. The solid lines represent the case that the Lagrangian of test particle preserves the scaling symmetry, and the dashed lines represent the case that the symmetry is not imposed. Left: EMDA; middle: KK; right: the lines in same color represent the KN, EMDA and KK cases respectively from left to right.

plot of Fig. 1, we observe that for the final STU black hole carrying a certain number of charges, the ISCO radius of the orbiting test particle gets smaller in the order of an STU black hole with four equal charges (KN), two equal charges (EMDA) and a single nonzero charge (KK). One can also understand the variation of the ISCO radius as due to the variation of the coupling constant β from zero to $\sqrt{3}$. We also plot the orbital angular momentum $\mathcal{L}_{\rm ISCO}/M$ against e in EMDA and KK cases in Fig. 2. First, as the charge to mass ratio varies from negative to positive, the angular momentum gradually decreases if the black hole carries nonzero charge. This can be understood physically as a result of the fact that an attractive electric force helps to increase the angular momentum while a repulsive one does the opposite. Second, we find that the angular momentum will be larger if the test particle is required to preserve the scaling symmetry in both KK and EMDA cases. As the final black hole carries more charges, the difference of the angular momentum between two cases corresponding to whether the symmetry is taken into account or not becomes larger. From the right plot of Fig. 2, we can see that for the final black hole that carries a certain number of charges, the angular momentum of the orbiting test particle becomes smaller in the order of STU black hole with four equal charges, two equal charges and a single nonzero charge. One can also attribute this decrease of the orbital angular momentum to the increase of the coupling constant β from zero to $\sqrt{3}$.

4.2. *Equal initial spins*

Now we apply the BKL recipe to estimate the final spin. In this subsection, we assume that the initial spins of the BBH are equal, i.e. $\chi_1 = \chi_2 = \chi$. According to Eq. (3.3), the final spin can be rewritten as

$$\mathcal{A}_f = \mathcal{L}\nu + M(1-2\nu)\chi\,. \tag{4.9}$$

Because we consider the merger of a BBH with weak charge, it is natural to consider the test particle carrying weak charge too. We set $e = 0.1$ for simplicity. (actually the test particle carrying different charges has similar behaviors, and so we do not consider the effect of the value of e on the final spin.) Given Q, χ and ν, we can solve the final spin. We plot $\mathcal{A}_f$ against ν for different initial spins χ from zero to 0.98 ($\chi = 0$ and $\chi = 0.98$ represent a non-spinning black hole and a near extreme black hole, i.e. a rapidly-spinning black hole, respectively) and different charges

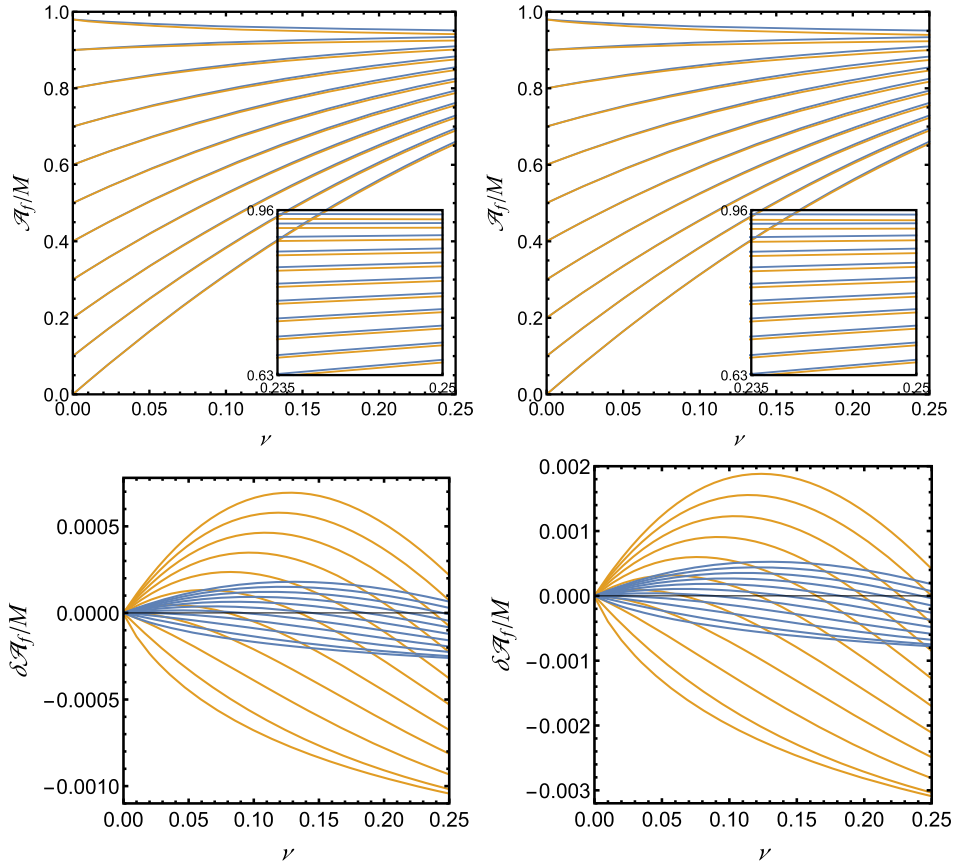

Fig. 3. The blue and orange lines represent $Q = 0.05M$ and $Q = 0.1M$ cases respectively. We set $e = 0.1$. Top: The final spin of the remnant black hole with unit mass against ν in the EMDA (left) and KK (right) cases. The initial spin χ of the lines in same color is 0, 0.1, 0.2, 0.3, 0.4, 0.5, 0.6, 0.7, 0.8, 0.9, 0.98 respectively from bottom to top. Bottom: the final spin's differences $\delta\mathcal{A}_f$ of remnant black holes between the two cases corresponding to the symmetry is taken into account or not in EMDA (left) and KK (right) cases. The initial spin χ of the lines in same color is 0, 0.1, 0.2, 0.3, 0.4, 0.5, 0.6, 0.7, 0.8, 0.9, 0.98 respectively from top to bottom.

$Q = 0.05M$ and $0.1M$ in Fig. 3 respectively. Notice that $\nu \sim 0$ and 0.25 represent the extreme initial mass ratio and equal initial masses respectively.

From the top plots in Fig. 3, we find that some features of the final spin estimated by the BKL recipe while the symmetry is imposed in the binary charged black hole merger case are similar to that in the neutral case [12] and charged case in which the symmetry is not taken into account [25]. First, the largest final spin for the remnant black hole is achieved for a binary extreme black hole merger with extreme initial mass ratio, which can be viewed as a charged particle falling into a charged rapidly-spinning black hole, regardless of the amount of charge carried by black hole. Besides, regardless of the amount of charges carried by the binary system, the final spin for the merger of binary non-spinning charged black holes with extremely high mass ratios is zero. Third, there is a critical value for the initial spins, below which, as the mass ratio approaches that of the equal-mass case ($\nu = 0.25$), the final spin increases. And above the

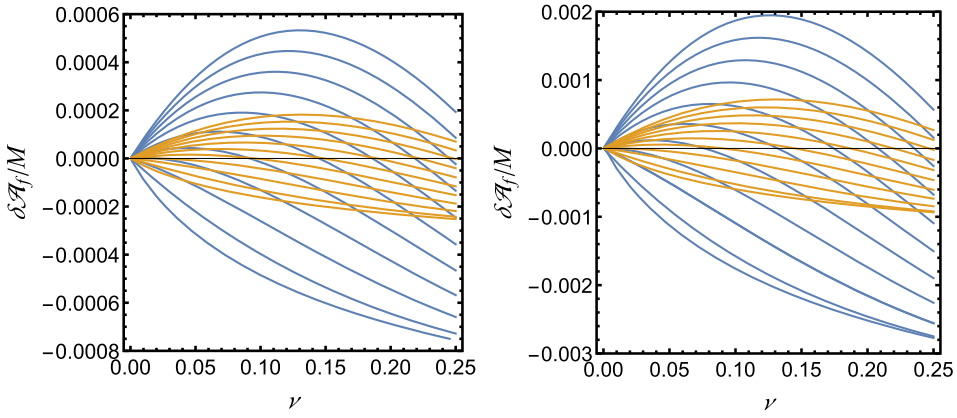

Fig. 4. Left: $Q = 0.05M$; right: $Q = 0.1M$. The blue line represents the final spin's difference $\delta\mathcal{A}_f$ of the remnant KK black hole (STU black hole with single charge) and KN black hole (STU black hole with four equal charges). The orange line represents the final spin's difference $\delta\mathcal{A}_f$ of the remnant EMDA black hole (STU black hole with two equal charges) and KN black hole (STU black hole with four equal charges). We set $e = 0.1$. The initial spins χ of the lines in same color are 0, 0.1, 0.2, 0.3, 0.4, 0.5, 0.6, 0.7, 0.8, 0.9 respectively from top to down.

critical value, the final spin decreases as ν increases. Fourth, the final spin will be smaller as the BBH system carries more charges.

From the bottom plots in Fig. 3, we find some subtle differences between two cases corresponding to whether the symmetry is taken into account or not. First, there is no difference between the two cases if the initial mass ratio is extreme. Second, while the initial black holes are non-spinning, the final spin estimated by the BKL recipe in which the symmetry is imposed is always larger than that in which the symmetry is not taken into account. The difference increases firstly and then decreases as the initial mass ratio approaches unity. Third, there is a threshold for the initial spins, above which, the final spin estimated by the BKL recipe in which the symmetry is imposed is always smaller than that in which the symmetry is not taken into account. All these features exist in different charge configurations of STU supergravity (both the KK and EMDA cases). It is worth comparing the final spin given by the BKL recipe with numeric simulations [34], and exploring if the BKL recipe could provide more accurate prediction of the final spin by requiring that the Lagrangian of the test particle preserves the scaling symmetry in supergravity.

We also study the final spin's difference $\delta\mathcal{A}_f$ between different charge configurations of STU supergravity with a certain small number of charges. To be specific, we plot the final spin's difference between the KK and KN black holes, and between the EMDA and KN black holes in Fig. 4. We find that the final spin's differences between the cases of different charge configurations have similar features as that between two cases corresponding to whether the scaling symmetry is taken into account or not. As mentioned in previous subsection, the difference can be also explained by the coupling constant in STU supergravity. First, there is no difference between the cases of different charge configurations (different coupling constant) if the initial mass ratio is extreme. Second, while the initial spins are zero, the final spin in the case of the single charge configuration (the coupling constant is $\sqrt{3}$) is always larger than that in the cases of other charge configurations (the coupling constant is smaller than $\sqrt{3}$). The difference increases firstly and then decreases as the equal mass limit is approached. Third, there is also a critical value for the initial spins, above which, the final spin in the case of the single charge configuration (the cou-

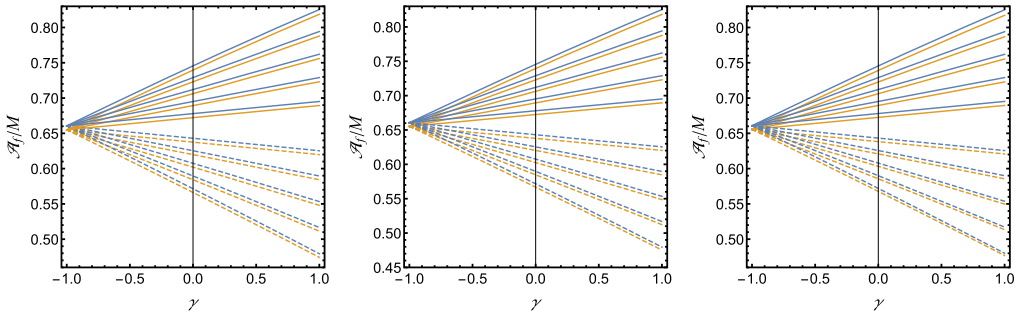

Fig. 5. Left: KN; middle: EMDA; right: KK. We set $e = 0.1$ for simplicity. The blue lines and orange lines represent $Q = 0.05M$ and $Q = 0.1M$ cases respectively. The solid lines and dashed lines represent positive and negative initial spin χ respectively. The value of χ of the lines in same color is 0.5, 0.4, 0.3, 0.2, 0.1, -0.1, -0.2, -0.3, -0.4, -0.5 respectively from top to bottom.

pling constant is $\sqrt{3}$) is always smaller than that in the cases of other charge configurations (the coupling constant is smaller than $\sqrt{3}$). The difference decreases gradually as the initial mass ratio approaches unity. All these results may provide a potential way to test different supergravites near strong gravitational regimes. Let us note that the final spin's difference between the two cases corresponding to whether the symmetry is taken into account or not is small because we only study the merger of a BBH with weak charges according to previous astronomical observations. If we consider the merger of a BBH with a greater amount of charges (we plot this case in the appendix B), the difference would become large similar to the result in [25]. We hope that the final spin's difference could be detected by future precise detectors, and could be used to test supergravities.

4.3. *Unequal initial spins*

In the previous works [25,26], the final spin estimation of the charged BBH merger was only considered in the equal initial spins case. Here, we will estimate the final spin of the BBH merger with unequal initial spins, i.e. $\chi_1 = \chi$, $\chi_2 = \gamma\chi$, in this subsection, and study the generic case in next subsection. Now, the final spin estimation formula can be rewritten as:

$$\mathcal{A}_f = \frac{1}{4}(\mathcal{L} + M\chi + \gamma M\chi)\,. \tag{4.10}$$

For simplicity, we assume that the initial black holes have equal masses ($\nu = 1/4$), weak charges ($Q = 0.05M$ and $0.1M$) and small spins $|\chi_i| \leq 0.5$. From the above equation, it follows that if the initial spins of two black holes are equal and opposite, the final spin is determined totally by the angular momentum $\mathcal{L}$ of the test particle regardless of the initial spins. The final spin increases when χ is positive and decreases when χ is negative. We plot the final spin A_f against initial spin ratio γ for different initial spins in the EM, EMDA and KK cases in Fig. 5. We impose that the test particle preserves the symmetry in all cases. Note that similar behaviors occur in the cases where the symmetry is not taken into consideration, So, we do not plot them here. From Fig. 5, we find that the final spin will be smaller as the BBH system carries more charges, which is same as that in the equal spin configuration. These properties exist in all cases irrespective of whether the test particle preserves the symmetry or not. We also study the difference of the final spin between two cases corresponding to whether the test particle preserves symmetry or not, and

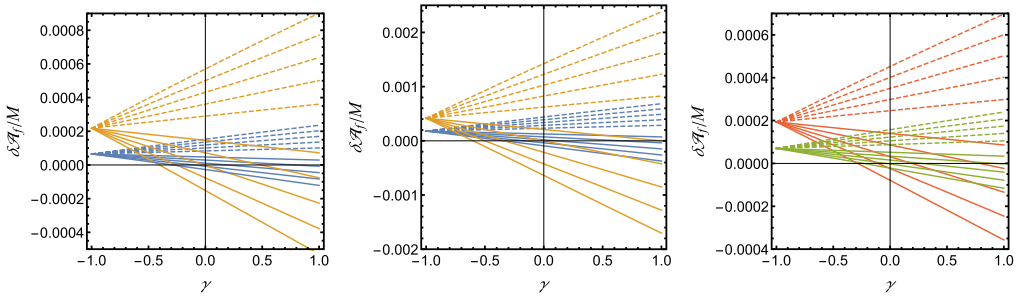

Fig. 6. In left and middle plots, the final spin's difference between two cases corresponding to whether the symmetry is taken into account or not in the EMDA (left) and KK (middle) theories. The blue lines and orange lines represent $Q = 0.05M$ and $Q = 0.1M$ respectively. In right plot the green lines and red lines represent the final spin's difference between the KK and KN cases and between the EMDA and KN cases. In right plot, the symmetry is taken into account and the charge $Q = 0.05M$. We set $e = 0.1$. The initial spin χ of the lines in same color is 0.5, 0.4, 0.3, 0.2, 0.1, -0.1, -0.2, -0.3, -0.4, -0.5 respectively from bottom to top.

plot the final spin's difference against γ in the EMDA and KK cases in Fig. 6. The difference is subtle. While the initial spins are opposite, the final spin estimated by the BKL recipe in which the symmetry is imposed is larger than that in which the symmetry is not imposed. For positive initial spins, the final spin estimated by BKL recipe in which the symmetry is imposed can be smaller than that in which the symmetry is not imposed.

4.4. Generic initial spins

In this subsection, we consider a more generic initial spin configuration, i.e. the orbit at the ISCO can be inclined with respect to the final total angular momentum. Following Ref. [12], we assume the initial masses, spins and unit orbital angular momentum $(M_1, M_2, \vec{S}_1, \vec{S}_2, \hat{L}_{\rm orb})$ at some point of the inspiral are known. On the other hand, we assume that the magnitude of the total spin $\vec{S}_{\rm tot} = \vec{S}_1 + \vec{S}_2$ and angle ϑ_{LS} between total spin and unit orbital angular momentum $\hat{L}_{\rm orb}$ remain constant. The total angular momentum $\vec{J}_f = M\mathcal{A}_f = \vec{L}_{\rm orb} + \vec{S}_{\rm tot}$, which could be written explicitly as [12]

$$L_{\rm orb}\cos\vartheta + S_{\rm tot}\cos(\vartheta_{LS} - \vartheta) = M\mathcal{A}_f\,, \tag{4.11}$$

$$L_{\rm orb}\sin\vartheta - S_{\rm tot}\sin(\vartheta_{LS} - \vartheta) = 0\,, \tag{4.12}$$

where $L_{\rm orb} = |\vec{L}_{\rm orb}|$ and $S_{\rm tot} = |\vec{S}_{\rm tot}|$. For simplicity, we adopt the simple fit formula given in Refs. [12,48,49]. The orbital angular momentum of the inclined orbit is given by

$$\mathcal{L} = \frac{1}{2}(1+\cos\vartheta)\mathcal{L}^{\rm pro} + \frac{1}{2}(1-\cos\vartheta)|\mathcal{L}^{\rm ret}|\,, \tag{4.13}$$

where ϑ is the inclination angle, representing the angle between final spin and the orbital angular momentum, and $\mathcal{L}^{\rm pro}$ and $\mathcal{L}^{\rm ret}$ represent the angular momentum of the prograde orbit and retrograde orbit respectively. Here we only consider the merger of a BBH with equal masses, spins and charges. The final spin can be rewritten as

$$\mathcal{A}_f = \frac{1}{8}\left(\mathcal{L}^{\rm pro} + |\mathcal{L}^{\rm ret}| + (\mathcal{L}^{\rm pro} - |\mathcal{L}^{\rm ret}|)\cos\vartheta\right)\left(\cos\vartheta + \frac{\cos(\vartheta_{LS}-\vartheta)}{\sin(\vartheta_{LS}-\vartheta)}\sin\vartheta\right). \tag{4.14}$$

We plot the final spin A_f against the total spin $S_{\rm tot}$ for different inclined angles ϑ_{LS} in the EM, EMDA and KK theories in Fig. 7 by requiring the particle to preserve the symmetry. Behaviors

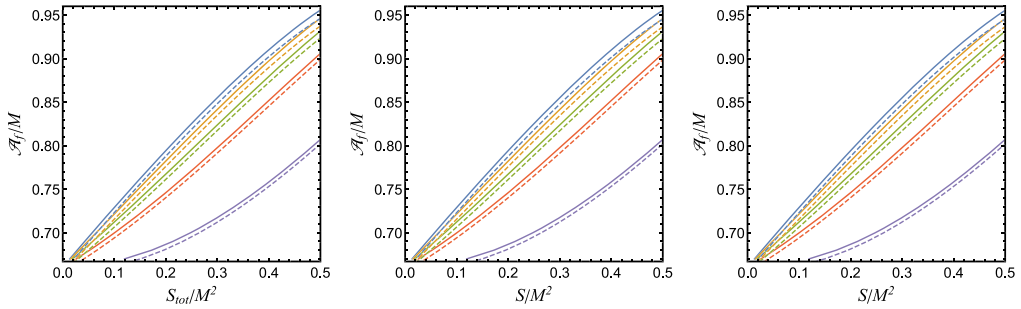

Fig. 7. The solid lines and dashed lines represent $Q = 0.05M$ and $Q = 0.1M$ respectively. Left: KN; middle: EMDA; right: KK. We set $e = 0.1$. The inclined angle in solid lines or dashed lines are $0, 30°, 45°, 60°, 90°$ respectively from left to right.

are similar to those in the case when the particle is not required to preserve the symmetry. We do not plot them here. From Fig. 7, we find that the final spin will be smaller as the BBH system carries more charges which is again the same as the feature in equal spin configuration. Besides, we find that final spin increases as the inclined angle increases in all charge configurations.

5. Conclusion

In this work, we study the final spin of a BBH merger in the framework of STU supergravity by using the BKL recipe. Comparing with the previous work [25], we reconsider the contribution of the orbital angular momentum of the binary system to the final spin by requiring that the test particle preserves the scaling symmetry in Lagrangian of supergravity. As a first step to explore whether the revised method could improve the precision of the final spin estimation, we study the final spin's difference in different initial spin configurations. In the equal initial spin configuration, we find that the difference is subtle. First, there is no difference between the two cases corresponding to whether the symmetry is taken into account or not if the initial mass ratio is extreme. Second, for the static BBH merger, the final spin estimated by the BKL recipe in which the symmetry is imposed is always larger than that in which the symmetry is not imposed. The difference increases firstly and then decreases as the equal mass limit is approached. Third, there is also a critical value for the initial spins, above which, the final spin is always smaller. The difference decreases constantly as the equal mass limit is approached. All these features exist in the merger of a binary STU black hole with different charge configurations (both the KK and EMDA cases). We also study the final spin difference between different charge configurations of STU supergravity with a certain number of charges. We find that the final spin differences between the cases of different charge configurations have similar features as that between two cases corresponding to whether the symmetry is imposed or not. It is worth comparing, in the future, the final spin given by the BKL recipe with numeric simulations [34], and exploring if the BKL recipe could provide more accurate prediction of the final spin by requiring the Lagrangian of the test particle preserves the scaling symmetry in supergravity. Besides, our result may provide a potential way to test string theory and supergravities near strong gravitational field regimes. We also study the final spin of a charged BBH merger in a case with unequal initial spin configuration and an even more generic spin configuration which was not studied in previous works. We obtain results similar to the equal initial spin case.

Finally, it is worth noting that we can also extract extra information in the merger stage by studying the null geodesic orbits for massless particle, known as light ring, in the final black hole. For a massless particle, the geodesics is $e^{\beta\phi}g_{\mu\nu}\dot{x}^\mu\dot{x}^\nu = 0$ which could be obtained from Eq. (3.12). It is easy to see that the conformal factor $e^{\beta\phi}$ plays no role in the corresponding calculation. So the scaling symmetry has no effect at the ringdown stage, and we do not study the light ring in this work.

CRediT authorship contribution statement

Shou-Long Li: Formal analysis, Investigation, Software, Validation, Writing – original draft. **Wen-Di Tan:** Conceptualization, Data curation, Methodology, Validation. **Puxun Wu:** Project administration, Resources, Visualization, Writing – review & editing. **Hongwei Yu:** Funding acquisition, Project administration, Supervision, Writing – review & editing.

Declaration of competing interest

The authors declare that they have no known competing financial interests or personal relationships that could have appeared to influence the work reported in this paper.

Acknowledgements

We are grateful to H. Lü, Hao Wei, Lijing Shao and Bing Sun for useful discussions. S.L., W.T., P.W, and H.Y. were supported in part by the NSFC under Grants No. 12105098, No. 11947216, No. 11935009, No. 11690034, No. 11805063, No. 11775077, and No. 12075084, and the China Postdoctoral Science Foundation (No. 2019M662785).

Appendix A. Black hole solutions

The KK rotating black hole solution is given by

$$\begin{aligned} ds^2_{\rm KK} &= -\frac{\Delta(cdt - a\sin^2\theta d\phi)^2}{\sqrt{H}(s^2(r^2+a^2)+\rho^2)} + \sqrt{H}\Big[\frac{\rho^2}{\Delta}dr^2 + \rho^2 d\theta^2 \\ &\quad + \frac{\sin^2\theta(adt - c(r^2+a^2)d\phi)^2}{s^2(r^2+a^2)+\rho^2}\Big], \\ A &= \frac{2mrs}{\rho^2+2mrs^2}(cdt - a\sin^2\theta d\phi)\,, \quad \varphi = -\frac{\sqrt{3}}{2}\ln H\,, \quad H = 1 + \frac{2rms^2}{\rho^2}\,, \end{aligned} \tag{A.1}$$

where $\hat{\mathcal{A}}^2 = A$, $\hat{A}_1 = \hat{A}_2 = \hat{\mathcal{A}}^1 = 0$, $\varphi_1 = \varphi_2 = \varphi_3 = \varphi/\sqrt{3}$, $\psi_1 = \psi_2 = \psi_3 = 0$. The parameters (m, δ, a) can be written in terms of the physical quantities M, Q, and $\mathcal{A} = J/M$ as

$$\begin{aligned} m &= \frac{3M}{2} - \frac{1}{2}\sqrt{M^2+8Q^2}\,, \\ c^2 &= \frac{M^2+2Q^2+M\sqrt{M^2+8Q^2}}{2(M^2-Q^2)}\,, \\ a &= \frac{\sqrt{2}M\mathcal{A}}{(M^2-4Q^2+M\sqrt{M^2+8Q^2})^{1/2}}\,, \end{aligned} \tag{A.2}$$

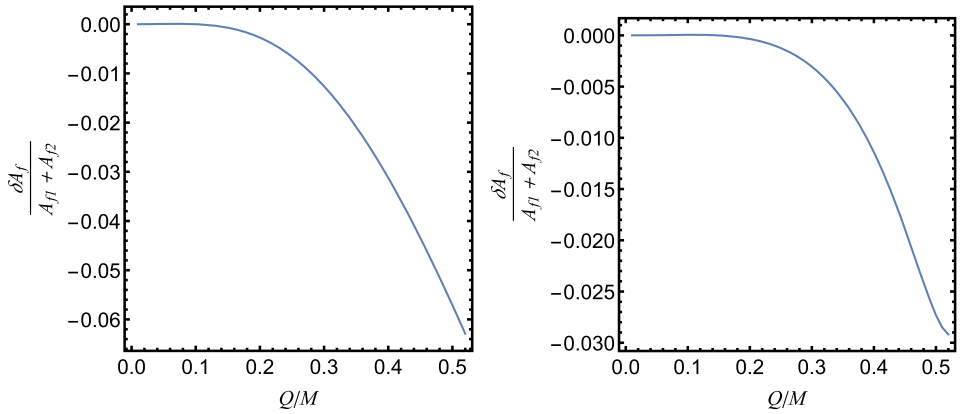

Fig. 8. Left: KK; right: EMDA. We set $e = 0.1$, initial spins $\chi = 0.1$, and consider the initial black holes have equal masses ($\nu = 1/4$).

where $Q \leq M$.

The EMDA rotating black hole solution is given by

$$
\begin{aligned}
ds^2 &= -\frac{\rho^2 - 2mr}{\rho^2 H}\left(dt + \frac{2mrac^2 \sin^2\theta d\phi}{\rho^2 - 2mr}\right)^2 + \rho^2 H\left(\frac{dr^2}{\Delta} + d\theta^2 + \frac{\Delta \sin^2\theta}{\rho^2 - 2mr}d\phi^2\right), \\
A &= \frac{2\sqrt{2}mrsc}{\rho^2 + 2mrs^2}(dt - a\sin^2\theta\, d\phi), \quad \varphi = -\ln H, \quad \psi = \frac{2ma\cos\theta s^2}{\rho^2}, \\
\hat{A}_1 &= \hat{\mathcal{A}}^1 = 0, \quad \varphi_2 = \varphi_3 = 0, \quad \psi_2 = \psi_3 = 0,
\end{aligned} \tag{A.3}
$$

where the parameters (m, δ, a) can be written as

$$
m = M - \frac{2Q^2}{M}, \quad a = \mathcal{A}, \quad c^2 = \frac{M^2}{M^2 - 2Q^2}, \tag{A.4}
$$

where $Q \leq \frac{\sqrt{2}}{2}M$.

The KN black hole solution is given by

$$
\begin{aligned}
ds^2 &= -\frac{\Delta_r}{\rho^2}(dt - a\sin^2\theta d\phi)^2 + \frac{\rho^2}{\Delta_r}dr^2 + \rho^2 d\theta^2 + \frac{\sin^2\theta}{\rho^2}(adt - (r^2 + a^2)d\phi)^2, \\
A &= \frac{4Qr}{\rho^2}(dt - a\sin^2\theta d\phi), \quad \Delta_r = r^2 - 2Mr + a^2 + 4Q^2.
\end{aligned} \tag{A.5}
$$

Appendix B. Final spin of BBH with large charges

In this appendix, we would like to show that our approach will provide some manifestly different results if we consider the merger of binary charged black hole with large charges. In Figs. 8, we plot the final spin's difference $\delta\mathcal{A}_f/(\mathcal{A}_{f1} + \mathcal{A}_{f2})$ between the two cases that the scaling symmetry is taken into account or not verse the electric charge Q in both KK and EMDA black holes where $\mathcal{A}_{f1}$ represents the symmetry is taken into account and $\mathcal{A}_{f2}$ represents the symmetry is not taken into account. We find the difference is about 6% and 3% in KK and EMDA black holes with charge $Q \approx 0.52M$ respectively.

References

[1] L. Blanchet, Gravitational radiation from post-Newtonian sources and inspiralling compact binaries, Living Rev. Relativ. 17 (2014) 2, https://doi.org/10.12942/lrr-2014-2, arXiv:1310.1528 [gr-qc].

[2] T. Regge, J.A. Wheeler, Stability of a Schwarzschild singularity, Phys. Rev. 108 (1957) 1063, https://doi.org/10.1103/PhysRev.108.1063.

[3] F.J. Zerilli, Gravitational field of a particle falling in a Schwarzschild geometry analyzed in tensor harmonics, Phys. Rev. D 2 (1970) 2141, https://doi.org/10.1103/PhysRevD.2.2141.

[4] S.A. Teukolsky, Perturbations of a rotating black hole. 1. Fundamental equations for gravitational electromagnetic and neutrino field perturbations, Astrophys. J. 185 (1973) 635, https://doi.org/10.1086/152444.

[5] S.A. Teukolsky, W.H. Press, Perturbations of a rotating black hole. III. Interaction of the hole with gravitational and electromagnetic radiation, Astrophys. J. 193 (1974) 443, https://doi.org/10.1086/153180.

[6] L. Lehner, F. Pretorius, Numerical relativity and astrophysics, Annu. Rev. Astron. Astrophys. 52 (2014) 661, https://doi.org/10.1146/annurev-astro-081913-040031, arXiv:1405.4840 [astro-ph.HE].

[7] B.P. Abbott, et al., LIGO Scientific Virgo Collaborations, Observation of gravitational waves from a binary black hole merger, Phys. Rev. Lett. 116 (6) (2016) 061102, https://doi.org/10.1103/PhysRevLett.116.061102, arXiv:1602.03837 [gr-qc].

[8] B.P. Abbott, et al., LIGO Scientific Virgo Collaborations, GW151226: observation of gravitational waves from a 22-solar-mass binary black hole coalescence, Phys. Rev. Lett. 116 (24) (2016) 241103, https://doi.org/10.1103/PhysRevLett.116.241103, arXiv:1606.04855 [gr-qc].

[9] B.P. Abbott, et al., LIGO Scientific VIRGO Collaborations, GW170104: observation of a 50-solar-mass binary black hole coalescence at redshift 0.2, Phys. Rev. Lett. 118 (22) (2017) 221101, https://doi.org/10.1103/PhysRevLett.118.221101, Erratum: Phys. Rev. Lett. 121 (12) (2018) 129901, https://doi.org/10.1103/PhysRevLett.121.129901, arXiv:1706.01812 [gr-qc].

[10] B.P. Abbott, et al., LIGO Scientific Virgo Collaborations, GW170608: observation of a 19-solar-mass binary black hole coalescence, Astrophys. J. 851 (2) (2017) L35, https://doi.org/10.3847/2041-8213/aa9f0c, arXiv:1711.05578 [astro-ph.HE].

[11] B.P. Abbott, et al., LIGO Scientific Virgo Collaborations, GW170814: a three-detector observation of gravitational waves from a binary black hole coalescence, Phys. Rev. Lett. 119 (14) (2017) 141101, https://doi.org/10.1103/PhysRevLett.119.141101, arXiv:1709.09660 [gr-qc].

[12] A. Buonanno, L.E. Kidder, L. Lehner, Estimating the final spin of a binary black hole coalescence, Phys. Rev. D 77 (2008) 026004, https://doi.org/10.1103/PhysRevD.77.026004, arXiv:0709.3839 [astro-ph].

[13] E. Barausse, L. Rezzolla, Predicting the direction of the final spin from the coalescence of two black holes, Astrophys. J. 704 (2009) L40, https://doi.org/10.1088/0004-637X/704/1/L40, arXiv:0904.2577 [gr-qc].

[14] E. Berti, J. Cardoso, V. Cardoso, M. Cavaglià, Matched-filtering and parameter estimation of ringdown waveforms, Phys. Rev. D 76 (2007) 104044, https://doi.org/10.1103/PhysRevD.76.104044, arXiv:0707.1202 [gr-qc].

[15] N.V. Krishnendu, K.G. Arun, C.K. Mishra, Testing the binary black hole nature of a compact binary coalescence, Phys. Rev. Lett. 119 (9) (2017) 091101, https://doi.org/10.1103/PhysRevLett.119.091101, arXiv:1701.06318 [gr-qc].

[16] A. Buonanno, T. Damour, Transition from inspiral to plunge in binary black hole coalescences, Phys. Rev. D 62 (2000) 064015, https://doi.org/10.1103/PhysRevD.62.064015, arXiv:gr-qc/0001013.

[17] T. Damour, A. Nagar, Final spin of a coalescing black-hole binary: an effective-one-body approach, Phys. Rev. D 76 (2007) 044003, https://doi.org/10.1103/PhysRevD.76.044003, arXiv:0704.3550 [gr-qc].

[18] A. Buonanno, Y. Pan, J.G. Baker, J. Centrella, B.J. Kelly, S.T. McWilliams, J.R. van Meter, Toward faithful templates for non-spinning binary black holes using the effective-one-body approach, Phys. Rev. D 76 (2007) 104049, https://doi.org/10.1103/PhysRevD.76.104049, arXiv:0706.3732 [gr-qc].

[19] A. Buonanno, G.B. Cook, F. Pretorius, Inspiral, merger and ring-down of equal-mass black-hole binaries, Phys. Rev. D 75 (2007) 124018, https://doi.org/10.1103/PhysRevD.75.124018, arXiv:gr-qc/0610122.

[20] M. Davis, R. Ruffini, W.H. Press, R.H. Price, Gravitational radiation from a particle falling radially into a Schwarzschild black hole, Phys. Rev. Lett. 27 (1971) 1466, https://doi.org/10.1103/PhysRevLett.27.1466.

[21] M. Davis, R. Ruffini, J. Tiomno, Pulses of gravitational radiation of a particle falling radially into a Schwarzschild black hole, Phys. Rev. D 5 (1972) 2932, https://doi.org/10.1103/PhysRevD.5.2932.

[22] R.H. Price, J. Pullin, Colliding black holes: the close limit, Phys. Rev. Lett. 72 (1994) 3297, https://doi.org/10.1103/PhysRevLett.72.3297, arXiv:gr-qc/9402039.

[23] J.G. Baker, A. Abrahams, P. Anninos, S. Brandt, R. Price, J. Pullin, E. Seidel, The collision of boosted black holes, Phys. Rev. D 55 (1997) 829, https://doi.org/10.1103/PhysRevD.55.829, arXiv:gr-qc/9608064.

[24] J.G. Baker, B. Bruegmann, M. Campanelli, C.O. Lousto, R. Takahashi, Plunge wave forms from inspiralling binary black holes, Phys. Rev. Lett. 87 (2001) 121103, https://doi.org/10.1103/PhysRevLett.87.121103, arXiv: gr-qc/0102037.
[25] P. Jai-akson, A. Chatrabhuti, O. Evnin, L. Lehner, Black hole merger estimates in Einstein-Maxwell and Einstein-Maxwell-dilaton gravity, Phys. Rev. D 96 (4) (2017) 044031, https://doi.org/10.1103/PhysRevD.96.044031, arXiv: 1706.06519 [gr-qc].
[26] H.M. Siahaan, Merger estimates for Kerr-Sen black holes, Phys. Rev. D 101 (6) (2020) 064036, https://doi.org/10.1103/PhysRevD.101.064036, arXiv:1907.02158 [gr-qc].
[27] D. Youm, Black holes and solitons in string theory, Phys. Rep. 316 (1999) 1, https://doi.org/10.1016/S0370-1573(99)00037-X, arXiv:hep-th/9710046.
[28] T. Mohaupt, Black holes in supergravity and string theory, Class. Quantum Gravity 17 (2000) 3429, https://doi.org/10.1088/0264-9381/17/17/303, arXiv:hep-th/0004098.
[29] A.W. Peet, TASI lectures on black holes in string theory, https://doi.org/10.1142/9789812799630_0003, arXiv: hep-th/0008241.
[30] H. Lü, C.N. Pope, K.S. Stelle, M theory / heterotic duality: a Kaluza-Klein perspective, Nucl. Phys. B 548 (1999) 87, https://doi.org/10.1016/S0550-3213(99)00086-3, arXiv:hep-th/9810159.
[31] E. Cremmer, B. Julia, H. Lü, C.N. Pope, Higher dimensional origin of $D = 3$ coset symmetries, arXiv:hep-th/9909099.
[32] D.D.K. Chow, G. Compère, Black holes in N=8 supergravity from SO(4, 4) hidden symmetries, Phys. Rev. D 90 (2) (2014) 025029, https://doi.org/10.1103/PhysRevD.90.025029, arXiv:1404.2602 [hep-th].
[33] H. Lü, Z.L. Wang, Q.Q. Zhao, Black holes that repel, Phys. Rev. D 99 (10) (2019) 101502, https://doi.org/10.1103/PhysRevD.99.101502, arXiv:1901.02894 [hep-th].
[34] E.W. Hirschmann, L. Lehner, S.L. Liebling, C. Palenzuela, Black hole dynamics in Einstein-Maxwell-dilaton theory, Phys. Rev. D 97 (6) (2018) 064032, https://doi.org/10.1103/PhysRevD.97.064032, arXiv:1706.09875 [gr-qc].
[35] F. Hofmann, E. Barausse, L. Rezzolla, The final spin from binary black holes in quasi-circular orbits, Astrophys. J. 825 (2) (2016) L19, https://doi.org/10.3847/2041-8205/825/2/L19, arXiv:1605.01938 [gr-qc].
[36] M.J. Duff, J.T. Liu, J. Rahmfeld, Four-dimensional string-string-string triality, Nucl. Phys. B 459 (1996) 125, arXiv: hep-th/9508094.
[37] Z.-W. Chong, M. Cvetič, H. Lü, C.N. Pope, Charged rotating black holes in four-dimensional gauged and ungauged supergravities, Nucl. Phys. B 717 (2005) 246, https://doi.org/10.1016/j.nuclphysb.2005.03.034, arXiv: hep-th/0411045.
[38] M. Cvetič, D. Youm, Entropy of nonextreme charged rotating black holes in string theory, Phys. Rev. D 54 (1996) 2612, https://doi.org/10.1103/PhysRevD.54.2612, arXiv:hep-th/9603147.
[39] A. Sen, Rotating charged black hole solution in heterotic string theory, Phys. Rev. Lett. 69 (1992) 1006–1009, https://doi.org/10.1103/PhysRevLett.69.1006, arXiv:hep-th/9204046 [hep-th].
[40] D. Rasheed, The rotating dyonic black holes of Kaluza-Klein theory, Nucl. Phys. B 454 (1995) 379–401, https://doi.org/10.1016/0550-3213(95)00396-A, arXiv:hep-th/9505038 [hep-th].
[41] V. Connaughton, et al., Fermi GBM observations of LIGO gravitational wave event GW150914, Astrophys. J. 826 (1) (2016) L6, https://doi.org/10.3847/2041-8205/826/1/L6, arXiv:1602.03920 [astro-ph.HE].
[42] A. Loeb, Electromagnetic counterparts to black hole mergers detected by LIGO, Astrophys. J. 819 (2) (2016) L21, https://doi.org/10.3847/2041-8205/819/2/L21, arXiv:1602.04735 [astro-ph.HE].
[43] R. Perna, D. Lazzati, B. Giacomazzo, Short gamma-ray bursts from the merger of two black holes, Astrophys. J. 821 (1) (2016) L18, https://doi.org/10.3847/2041-8205/821/1/L18, arXiv:1602.05140 [astro-ph.HE].
[44] B. Zhang, Mergers of charged black holes: gravitational wave events, short gamma-ray bursts, and fast radio bursts, Astrophys. J. 827 (2) (2016) L31, https://doi.org/10.3847/2041-8205/827/2/L31, arXiv:1602.04542 [astro-ph.HE].
[45] S.E. Woosley, The progenitor of GW150914, Astrophys. J. 824 (1) (2016) L10, https://doi.org/10.3847/2041-8205/824/1/L10, arXiv:1603.00511 [astro-ph.HE].
[46] T. Liu, G.E. Romero, M.L. Liu, A. Li, Fast radio bursts and their Gamma-ray or radio afterglows as Kerr–Newman black hole binaries, Astrophys. J. 826 (1) (2016) 82, https://doi.org/10.3847/0004-637X/826/1/82, arXiv: 1602.06907 [astro-ph.HE].
[47] M. Kesden, Can binary mergers produce maximally spinning black holes?, Phys. Rev. D 78 (2008) 084030, https://doi.org/10.1103/PhysRevD.78.084030, arXiv:0807.3043 [astro-ph].
[48] S.A. Hughes, R.D. Blandford, Black hole mass and spin coevolution by mergers, Astrophys. J. 585 (2003) L101, https://doi.org/10.1086/375495, arXiv:astro-ph/0208484.
[49] S.W. Wei, Y.X. Liu, Merger estimates for rotating Kerr black holes in modified gravity, Phys. Rev. D 98 (2) (2018) 024042, https://doi.org/10.1103/PhysRevD.98.024042, arXiv:1803.09530 [gr-qc].